G Model
MRC-3111; No. of Pages 5

ARTICLE IN PRESS

Mechanics Research Communications xxx (2016) xxx–xxx

Contents lists available at ScienceDirect

Mechanics Research Communications

journal homepage: www.elsevier.com/locate/mechrescom

Pantographic structures presenting statistically distributed defects: Numerical investigations of the effects on deformation fields

Emilio Turco[a,*], Nicola Luigi Rizzi[b]

[a] Department of Architecture, Design and Urban planning (DADU), University of Sassari, Italy
[b] Department of Architecture, University of Roma Tre, Italy

ARTICLE INFO

Article history:
Received 15 August 2016
Accepted 17 September 2016
Available online xxx

MSC:
74-XX
70H03
74-04
74B20
74S30
74Q05

Keywords:
Pantographic structures
Statistically distributed defects
Lagrangian model
Micro-mechanical model
Large displacements

ABSTRACT

In 3D printing process, when small length scales are attained, it is more frequent the onset of imperfections. In the present paper it is studied how the performances of pantographic structures (as defined and introduced in dell'Isola et al. (2005) [1]) are affected by statistically distributed defects. The relevance of the treated problem is more cogent as the technological tools now available allow for the construction of more and more miniaturised fabrics constituted by beam lattices. Our simulations show that in presence of defects following a (truncated) Gaussian distribution the performances of planar pantographic sheets remain qualitatively the same, even if some relevant negative quantitative effects may occur.

1. Introduction

In [1,2] the idea of pantographic sheet is proposed. This concept was explored in some theoretical papers [3–5] and experimentally in a series of papers started by [1]. The new frontiers in the theory of metamaterials are located in the direction of miniaturisation. It is nowadays trendy to consider nanostructures, nanomachines or nanosystems (following the ideas presented in Feynman's classic 1959 talk: There's Plenty of Room at the Bottom, http://www.imss.caltech.edu). The pantographic sheets (and all their conceivable and hopefully useful generalisations) could be an interesting part of the fabric constituting exotic metamaterials. This means that their performances, and in particular their most interesting properties (see, *e.g.*, [1]), must be stable under the (possibly small) variation of the geometrical structure of the fabric and of the mechanical properties of the constituting material. Of course a careful and rigorous sensitivity analysis must be conceived and performed in order to answer satisfactorily to the demands of precision requested to transform the concept into a technological solution. The present paper gives a preliminary and positive indication about the "good behaviour" of pantographic structure in presence of randomly distributed defects. This means that there is a strong motivation in developing more sophisticated methods and in performing a further measurements campaign.

2. Numerical model *á la* Hencky

Here we give the basic assumptions and the definitions of the strain energy for an *imperfect*, this term will be better clarified below, pantographic structure, *i.e.* with an assemblage of beams following two directions and interconnected by pivots. In [6,7] a mechanical model derived from the work of Hencky was presented and its numerical results, when large displacements are considered, thoroughly discussed. The Hencky-type mechanical model is based on, and completely defined by, the strain energy in terms of the current position of each mass (here we suppose the mass concentrated

* Corresponding author.
E-mail addresses: emilio.turco@uniss.it (E. Turco), nicolaluigi.rizzi@uniroma3.it (N.L. Rizzi).

http://dx.doi.org/10.1016/j.mechrescom.2016.09.006
0093-6413/

Please cite this article in press as: E. Turco, N.L. Rizzi, Pantographic structures presenting statistically distributed defects: Numerical investigations of the effects on deformation fields, Mech. Re. Commun. (2016), http://dx.doi.org/10.1016/j.mechrescom.2016.09.006

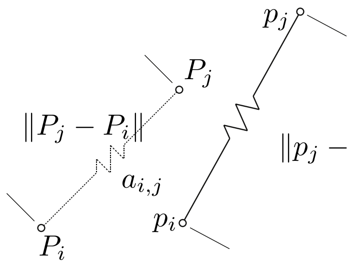

Fig. 1. Axial spring: kinematic.

in the pivot positions). An axial spring, which connects two masses, stores elastic energy which depends, quadratically, on its length variation:

$$w_a = \frac{1}{2} a_{i,j} \left(\|p_j - p_i\| - \|P_j - P_i\| \right)^2, \tag{1}$$

where p_i and p_j are the current position of the particles distinguished by their positions P_i and P_j in the reference configuration and connected by an extensional spring whose stiffness is denoted $a_{i,j}$, see Fig. 1.

A bending spring expresses the interaction on three particles P_i, P_j and P_k, see Fig. 2; it stores energy which depends on the angle $\beta_{i,j,k}$ formed by the two segments p_ip_j and p_jp_k in the actual configurations:

$$w_b = \frac{1}{2} b_{i,j,k} (\beta_{i,j,k} - \beta^{(0)}_{i,j,k})^2, \tag{2}$$

where $\beta^{(0)}_{i,j,k}$ is the angle formed by the two segments P_iP_j and P_jP_k and $b_{i,j,k}$ denote the stiffness of the bending spring. We remark that both angles $\beta_{i,j,k}$ and $\beta^{(0)}_{i,j,k}$ can easily be evaluated by using the Carnot's theorem both in the reference and in the current positions. It also to be noticed that the bending energy used here is different, even if entirely equivalent, from that used in [6].

Shear springs interact elastically *via* the interconnecting pivots between the segment p_ip_j and p_jp_k (in the current configuration), see Fig. 3: if $\sigma^{(0)}_{i,j,k}$ and $\sigma^{(0)}_{i,j,k}$ are the angles in the reference and current configuration, respectively, we assume that the stored energy is:

$$w_s = \frac{1}{2} s_{i,j,k} (\sigma_{i,j,k} - \sigma^{(0)}_{i,j,k})^2, \tag{3}$$

where $s_{i,j,k}$ is the stiffness of the shear spring and the angles $\sigma^{(0)}_{i,j,k}$ and $\sigma_{i,j,k}$ can be evaluated again by using the Carnot's theorem in both reference and current configurations.

The total potential energy is simply computed summing each single term defined in the foregoing. From the energy it is possible, in a straightforward manner, to compute its gradient, the internal force vector, and the Hessian, the tangent stiffness matrix. Gradient and Hessian are the basic ingredient for the step-by-step procedure

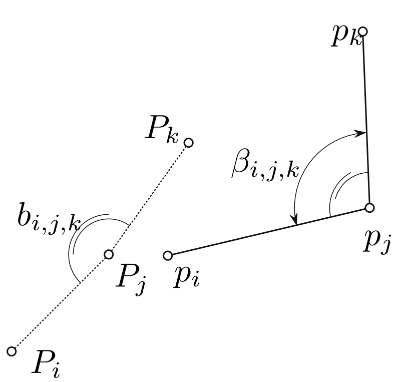

Fig. 2. Bending spring: kinematic.

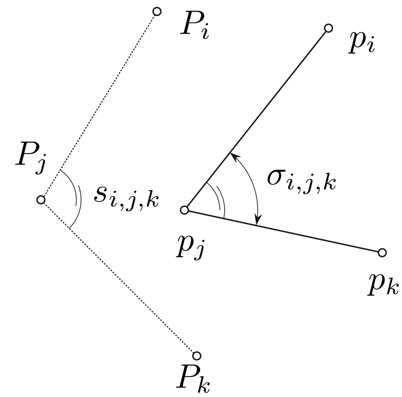

Fig. 3. Shear spring: kinematic.

which reconstructs the complete nonlinear equilibrium path by using an incremental-iterative procedure, guided by the imposed displacements, based on the classic Newton's residual scheme. The interested reader will find a thoroughly description of the Hencky-model (even if the bending part is here different) and some insights about the numerical code implementation in [6,7].

The *imperfect* pantographic structure is defined starting from the perfect one. This last is defined by the five geometrical parameters: $\ell_1, \ell_2, \alpha_1, \alpha_2, \varepsilon$, see Fig. 4, and by the three spring stiffnesses $a_{i,j}$, $b_{i,j,k}$ and $s_{i,j,k}$. This choice could be easily generalized, for example, considering the stiffness of the elongation and bending springs different in α_1- and α_2-directions.

The imperfect pantographic structure is obtained from the perfect one modifying some of the defined parameters in a statistically way. The first choice possible, and that has some pretty interesting application outcomes, is the modification of the reference positions of the masses: each position P_i, in the perfect system, is moved in the position $\tilde{P}_i$, in the imperfect system, in such a way that $\|\tilde{P}_i - P_i\| < \rho_g \varepsilon$ being ρ_g a parameter which represents the size of the geometric defect. The position $\tilde{P}_i$ can be generated by using a standard generator of pseudo-random numbers extracted from the preferred distribution (*e.g.* the one that models better the construction errors of the artefacts). For example, the case $\ell_1 = \ell_2 = 100$, $\alpha_1 = \pi/4$, $\alpha_2 = 3\pi/4$, $\varepsilon = 10/\sqrt{2}$ and $\rho_g = 0.25$ produces, starting from that shown in Fig. 4, the geometrically imperfect associated pantographic structure reported in Fig. 5. Defects concerning stiffness parameters can be modeled exactly in the same way. For example, the axial stiffness parameter $a_{i,j}$ becomes $\tilde{a}_{i,j} = (1 + \rho_a) a_{i,j}$ being $-1 < \rho_a$ a pseudo-random number extracted from the preferred distribution on the basis of the statistical information on the defects of the artefacts.

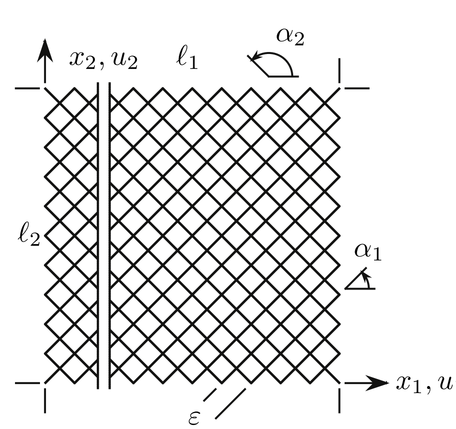

Fig. 4. Geometrically *perfect* pantographic structure.

Please cite this article in press as: E. Turco, N.L. Rizzi, Pantographic structures presenting statistically distributed defects: Numerical investigations of the effects on deformation fields, Mech. Re. Commun. (2016), http://dx.doi.org/10.1016/j.mechrescom.2016.09.006

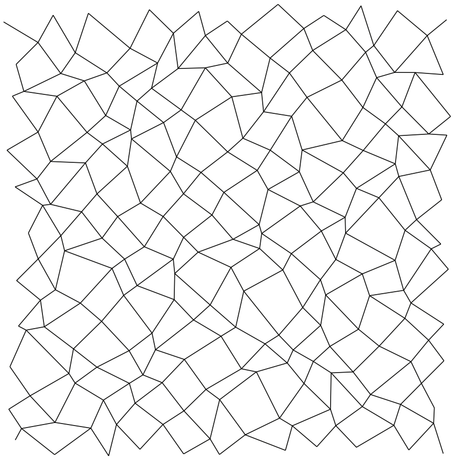

Fig. 5. Geometrically *imperfect* associated pantographic structure ($\rho_g = 0.25$).

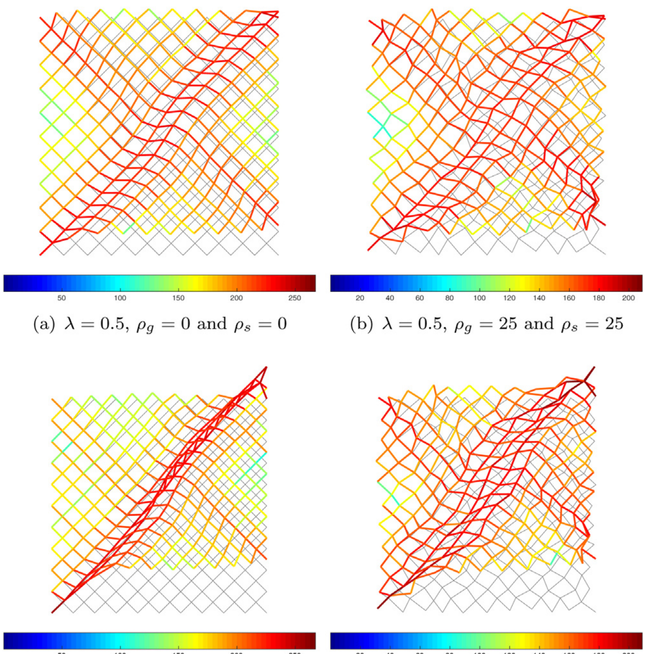

(a) $\lambda = 0.5$, $\rho_g = 0$ and $\rho_s = 0$ (b) $\lambda = 0.5$, $\rho_g = 25$ and $\rho_s = 25$

(c) $\lambda = 1$, $\rho_g = 0$ and $\rho_s = 0$ (d) $\lambda = 1$, $\rho_g = 25$ and $\rho_s = 25$

Fig. 6. Shear test: deformation for $\lambda = 0.5$, 1 for the perfect (on the left) and the imperfect (on the right) varying λ (colors represent the strain energy density). (For interpretation of reference to color in this figure legend, the reader is referred to the web version of this article.)

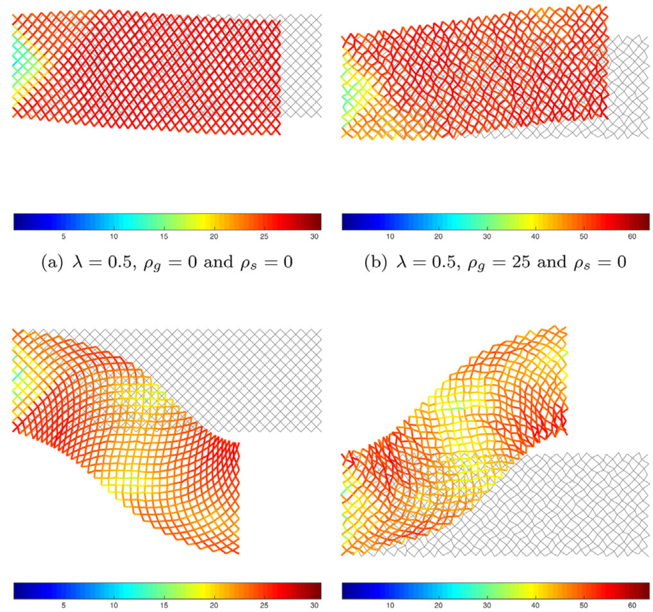

(a) $\lambda = 0.5$, $\rho_g = 0$ and $\rho_s = 0$ (b) $\lambda = 0.5$, $\rho_g = 25$ and $\rho_s = 0$

(c) $\lambda = 1$, $\rho_g = 0$ and $\rho_s = 0$ (d) $\lambda = 1$, $\rho_g = 25$ and $\rho_s = 0$

Fig. 8. Compression test: deformation for $\lambda = 0.5$, 1 for the perfect (on the left) and the imperfect (on the right) varying λ (colors represent the strain energy density). (For interpretation of reference to color in this figure legend, the reader is referred to the web version of this article.)

3. Numerical simulation

Among many numerical simulations performed we report here two cases: the first one is inspired by a shear test on a square specimen and the second one to a compression test on a rectangular specimen. In both tests we assume that the defect amplitude parameter for the geometry, defined in the foregoing, is $\rho_g = 0.25$ while we assume $\rho_a = \rho_b = \rho_s = 0.25$ for the first test and $\rho_a = \rho_b = \rho_s = 0$ for the second one. The pseudo-random numbers necessary to build the imperfect system are all extracted from the standard uniform distribution.

3.1. Shear test

We consider the case of a square specimen with side equal to 100 mm; furthermore we assume that the left vertical side is completely locked and on the right vertical side there is an imposed vertical displacement equal to 25 mm (the horizontal one is null). The numerical simulation of this problem gives the deformation

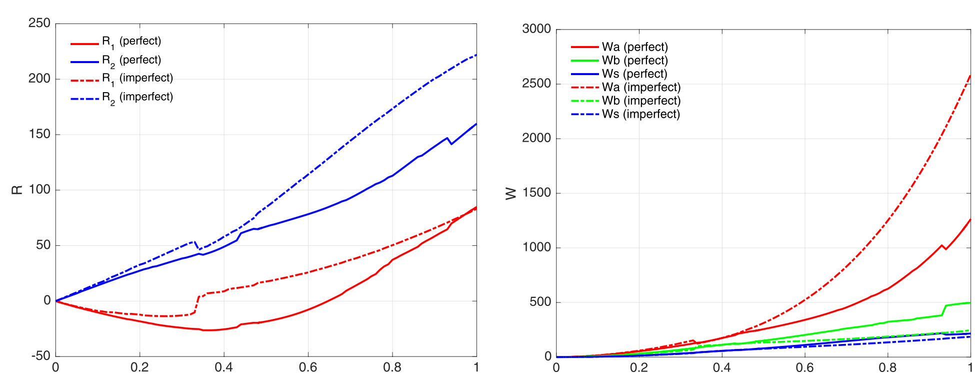

(a) Global structural reaction R (b) Strain energy W

Fig. 7. Shear test: global structural reaction R and strain energy W *vs.* λ.

Please cite this article in press as: E. Turco, N.L. Rizzi, Pantographic structures presenting statistically distributed defects: Numerical investigations of the effects on deformation fields, Mech. Re. Commun. (2016), http://dx.doi.org/10.1016/j.mechrescom.2016.09.006

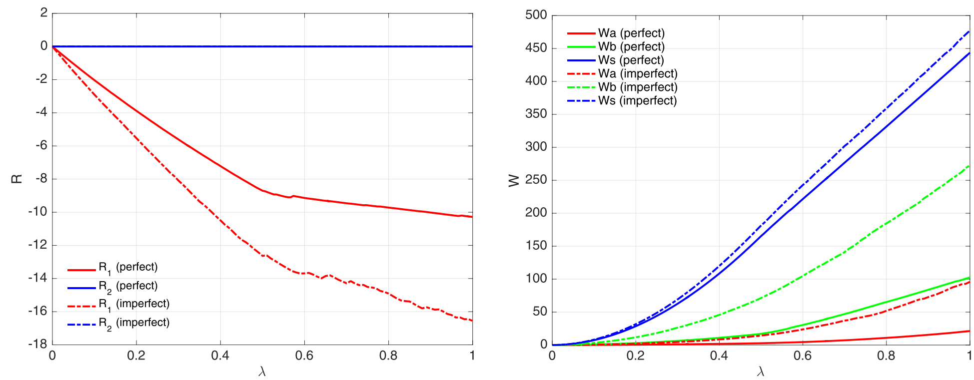

(a) Global structural reaction R (b) Strain energy W

Fig. 9. Compression test: global structural reaction R and strain energy W *vs.* λ.

history reported in Fig. 6 both for the perfect (on the left) and imperfect (on the right) structure. The non-dimensional displacement parameter λ was used to individuate the imposed displacement level ($\lambda = 1$ corresponds to 25 mm). Furthermore, in Fig. 7 there are the global structural reaction (on the left vertical side) and the energy (distinct for axial W_a, bending W_b and shear W_s) varying λ both for the perfect and imperfect structure. We underline that maximum levels of the strain energy are concentrated along the main diagonals of the square and not negligible variations between the perfect and imperfect system, both on R and W.

3.2. Compression test

For a rectangular specimen having the longer and the shorter side equal to 300 mm and 100 mm, respectively, assuming that the left vertical side is locked and on the right vertical side there is an imposed horizontal displacement equal to 80 mm (vertical displacements are free). Also in this case we performed the numerical simulation of the perfect and imperfect systems. Fig. 8 shows the deformation history both for the perfect (on the left) and imperfect (on the right) structure while Fig. 9 reports the global structural reaction (on the left) and the energy (on the right, associated to axial, bending and shear strain) both for perfect and imperfect structure. Deformations are distinct again by the non-dimensional displacement parameter ($\lambda = 1$ corresponds, in this case, to 80 mm). In this case we observed a rather evident buckling phenomenon both for the perfect and imperfect system. For the perfect one the final deformation derives from *numerical imperfections*, for the imperfect one derives from the modelled geometric imperfections.

4. Concluding remarks and future perspectives

It has to be remarked, once more, that Lagrangian modelling techniques supply a powerful tool of prediction and investigation of natural phenomena and technological devices. The "natural" discretisation they supply for the study of physical systems allows for an effective analysis of many study cases and, in perspective, of all technologically meaningful situations. In this paper we prove that, once basing our numerical analysis tools on discrete Lagrange equations, it is rather easy to confront the difficult problem of the study of inhomogeneous systems. Indeed without any relevant increase of calculation time (and with a simply adaptation of the numerical code previously formulated for "perfect" pantographic sheets) we can obtain useful predictions about the influence of random imperfections on their performances. The obtained results indicate a comforting stability of their most relevant mechanical features under even quantitatively significant variations of the geometric structure of the fabric: this means that systematic theoretical, numerical and experimental investigations are motivated. We remark that, although pantographic structures were conceived to give an example of second gradient metamaterial modeled as generalized continua, they give appreciable qualitative results using handy models, see, *e.g.*, [8–15]. However in some specific deformation phenomena, the most appropriate, or convenient, models could not be those deriving from continuous theory even if, as seen in [2,16], when the qualitative description of their behavior is needed, then second gradient continuum models are surely more convenient. Future challenges concern: (i) the extension of the Hencky-type model to granular media interactions, see [17], or to generalized continua, see [8,18,19] in general cases and [20,21] for some interesting applications; (ii) the generalization of the Hencky-type model, in order to design even more complex metamaterials, by using the NURBS interpolation to build complex systems of springs: see *e.g.* [22–29]; (iii) the identification of discrete model parameters, *i.e.* the stiffnesses of the springs, requires a targeted investigation. To this aim, it is necessary and useful an extended sensitivity analysis on these parameters and the use of the tools reported in the review paper [30] and, in a detailed form, in [31–35]; (iv) the extension to the dynamic field, see some deep insight in the review paper [36] and also [37,38] for general considerations on the spectrum; (v) the onset and the evolution of a failure mechanism for pantographic sheets involves both fibers and pivots rupture: a first attempt was presented in [39] obtaining an accurate result when the case of a failure mechanism concerning a fiber is considered. In this direction, it should also be considered the modeling of the out of plane deformation in such a way that buckling phenomena can be caught, see, *e.g.*, [40–46].

References

[1] F. dell'Isola, T. Lekszycki, M. Pawlikowski, R. Grygoruk, L. Greco, Designing a light fabric metamaterial being highly macroscopically tough under directional extension: first experimental evidence, Z. Angewandte Mathematik und Physik 66 (6) (2015) 3473–3498.
[2] F. dell'Isola, I. Giorgio, M. Pawlikowski, N.L. Rizzi, Large deformations of planar extensible beams and pantographic lattices: heuristic homogenisation, experimental and numerical examples of equilibrium, Proc. R. Soc. London A: Math. Phys. Eng. Sci. 472 (2185) (2016).
[3] J.-J. Alibert, P. Seppecher, F. dell'Isola, Truss modular beams with deformation energy depending on higher displacement gradients, Math. Mech. Solids 8 (1) (2003) 51–73.
[4] P. Seppecher, J.-J. Alibert, F. dell'Isola, Linear elastic trusses leading to continua with exotic mechanical interactions, in: Journal of Physics: Conference Series, volume 319(1), IOP Publishing, 2011, p. 012018.
[5] J.-J. Alibert, A. Della Corte, Second-gradient continua as homogenized limit of pantographic microstructured plates: a rigorous proof, Z. Angew. Math. Phys. (2015).
[6] E. Turco, F. dell'Isola, A. Cazzani, N.L. Rizzi, Hencky-type discrete model for pantographic structures: numerical comparison with second gradient continuum models, Z. Angew. Math. Phys. 67 (4) (2016) 1–28.

Please cite this article in press as: E. Turco, N.L. Rizzi, Pantographic structures presenting statistically distributed defects: Numerical investigations of the effects on deformation fields, Mech. Re. Commun. (2016), http://dx.doi.org/10.1016/j.mechrescom.2016.09.006

[7] E. Turco, M. Golaszewski, A. Cazzani, N.L. Rizzi, Large deformations induced in planar pantographic sheets by loads applied on fibers: experimental validation of a discrete Lagrangian model, Mech. Res. Commun. 76 (2016) 51–56.
[8] F. dell'Isola, D. Steigmann, A. Della Corte, Synthesis of fibrous complex structures: designing microstructure to deliver targeted macroscale response, Appl. Mech. Rev. 67 (6) (2015) 060804.
[9] I. Giorgio, R. Grygoruk, F. dell'Isola, D.J. Steigmann, Pattern formation in the three-dimensional deformations of fibered sheets, Mech. Res. Commun. 69 (2015) 164–171.
[10] D. Scerrato, I. Giorgio, N.L. Rizzi, Three-dimensional instabilities of pantographic sheets with parabolic lattices: numerical investigations, Z. Angew. Math. Phys. 67 (3) (2016) 1–19.
[11] D. Scerrato, I.A. Zhurba Eremeeva, T. Lekszycki, N.L. Rizzi, On the effect of shear stiffness on the plane deformation of linear second gradient pantographic sheets, Z. Angew. Math. Mech. (2016), http://dx.doi.org/10.1002/zamm.201600066.
[12] F. dell'Isola, A. Della Corte, L. Greco, A. Luongo, Plane bias extension test for a continuum with two inextensible families of fibers: a variational treatment with lagrange multipliers and a perturbation solution, Int. J. Solids Struct. 81 (2016) 1–12.
[13] M. Cuomo, F. dell'Isola, L. Greco, Simplified analysis of a generalized bias test for fabrics with two families of inextensible fibres, Z. Angew. Math. Phys. 67 (3) (2016) 1–23.
[14] F. dell'Isola, M. Cuomo, L. Greco, A. Della Corte, Bias extension test for pantographic sheets: numerical simulations based on second gradient shear energies, J. Eng. Math. (2016), http://dx.doi.org/10.1007/s10665-016-9865-7.
[15] L. Placidi, L. Greco, S. Bucci, E. Turco, N.L. Rizzi, A second gradient formulation for a 2D fabric sheet with inextensible fibres, Z. Angew. Math. Phys. (2016), http://dx.doi.org/10.1007/s00033-016-0701-8.
[16] F. dell'Isola, U. Andreaus, L. Placidi, At the origins and in the vanguard of peridynamics, non-local and higher-gradient continuum mechanics: an underestimated and still topical contribution of Gabrio Piola, Math. Mech. Solids 20 (8) (2015) 887–928.
[17] A. Misra, P. Poorsolhjouy, Granular micromechanics based micromorphic model predicts frequency band gaps, Contin. Mech. Thermodyn. 28 (1) (2016) 215–234.
[18] J. Altenbach, H. Altenbach, V.A. Eremeyev, On generalized Cosserat-type theories of plates and shells: a short review and bibliography, Arch. Appl. Mech. 80 (1) (2010) 73–92.
[19] K. Elnady, F. Dos Reis, J.-F. Ganghoffer, Construction of second order gradient continuous media by the discrete asymptotic homogenization method, Int. J. Appl. Mech. (2014).
[20] F. Tedesco, A. Bilotta, E. Turco, Multiscale 3D mixed FEM analysis of historical masonry constructions, Eur. J. Environ. Civil Eng. (2016), http://dx.doi.org/10.1080/19648189.2015.1134676.
[21] A. Tomic, A. Grillo, S. Federico, Poroelastic materials reinforced by statistically oriented fibres – numerical implementation and application to articular cartilage, IMA J. Appl. Math. 79 (2014) 1027–1059.
[22] A. Cazzani, M. Malagù, E. Turco, Isogeometric analysis of plane curved beams, Math. Mech. Solids 21 (5) (2016) 562–577.
[23] A. Cazzani, M. Malagù, E. Turco, Isogeometric analysis: a powerful numerical tool for the elastic analysis of historical masonry arches, Contin. Mech. Thermodyn. 28 (1) (2016) 139–156.
[24] A. Cazzani, M. Malagù, E. Turco, F. Stochino, Constitutive models for strongly curved beams in the frame of isogeometric analysis, Math. Mech. Solids 21 (2) (2016) 182–209.
[25] A. Bilotta, G. Formica, E. Turco, Performance of a high-continuity finite element in three-dimensional elasticity, International Journal for Numerical Methods in Biomedical Engineering 26 (2010) 1155–1175.
[26] L. Greco, M. Cuomo, B-Spline interpolation of Kirchhoff-Love space rods, Comput. Methods Appl. Mech. Eng. 256 (2013) 251–269.
[27] L. Greco, M. Cuomo, An implicit G^1 multi patch B-spline interpolation for Kirchhoff-Love space rod, Comput. Meth. Appl. Mech. Eng. 269 (2014) 173–197.
[28] L. Greco, M. Cuomo, An isogeometric implicit G1 mixed finite element for Kirchhoff space rods, Comput. Methods Appl. Mech. Eng. 298 (2016) 325–349.
[29] A. Cazzani, F. Stochino, E. Turco, An analytical assessment of finite elements and isogeometric analysis of the whole spectrum of Timoshenko beams, Z. Angew. Math. Mech. (2016) 1–25, http://dx.doi.org/10.1002/zamm.201500280.
[30] E. Turco, Tools for the numerical solution of inverse problems in structural mechanics: review and research perspectives, Eur. J. Environ. Civil Eng. (2016) 1–46, http://dx.doi.org/10.1080/19648189.2015.1134673.
[31] T. Lekszycki, N. Olhoff, J.J. Pedersen, Modelling and identification of viscoelastic properties of vibrating sandwich beams, Compos. Struct. 22 (1) (1992) 15–31.
[32] A. Bilotta, E. Turco, A numerical study on the solution of the Cauchy problem in elasticity, Int. J. Solids Struct. 46 (2009) 4451–4477.
[33] A. Bilotta, A. Morassi, E. Turco, Reconstructing blockages in a symmetric duct via quasi-isospectral horn operators, J. Sound Vib. 366 (2016) 149–172.
[34] A. Bilotta, E. Turco, Numerical sensitivity analysis of corrosion detection, Mathematics and Mechanics of Solids (2014) 1–17, http://dx.doi.org/10.1177/1081286514560093.
[35] E. Turco, Identification of axial forces on statically indeterminate pin-jointed trusses by a nondestructive mechanical test, Open Civil Eng. J. 7 (2013) 50–57.
[36] D. Del Vescovo, I. Giorgio, Dynamic problems for metamaterials: review of existing models and ideas for further research, Int. J. Eng. Sci. 80 (2014) 153–172.
[37] A. Cazzani, F. Stochino, E. Turco, On the whole spectrum of Timoshenko beams. Part I: a theoretical revisitation, Z. Angew. Math. Phys. 67 (24) (2016) 1–30.
[38] A. Cazzani, F. Stochino, E. Turco, On the whole spectrum of Timoshenko beams. Part II: further applications, Z. Angew. Math. Phys. 67 (25) (2016) 1–21.
[39] E. Turco, F. dell'Isola, N.L. Rizzi, R. Grygoruk, W.N. Müller, C. Liebold, Fiber rupture in sheared planar pantographic sheets: numerical and experimental evidence, Mech. Res. Commun. 76 (2016) 86–90.
[40] N. Rizzi, V. Varano, S. Gabriele, Initial postbuckling behavior of thin-walled frames under mode interaction, Thin-Walled Struct. 68 (2013) 124–134.
[41] S. Gabriele, N. Rizzi, V. Varano, A 1D higher gradient model derived from Koiter's shell theory, Math. Mech. Solids 6 (2014).
[42] H. AminPour, N. Rizzi, A one-dimensional continuum with microstructure for single-wall carbon nanotubes bifurcation analysis, Math. Mech. Solids 21 (2) (2016) 168–181.
[43] S. Gabriele, N.L. Rizzi, V. Varano, A 1D nonlinear TWB model accounting for in plane cross-section deformation, Int. J. Solids Struct. 94-95 (2016) 170–178.
[44] H. AminPour, N.L. Rizzi, On the continuum modelling of carbon nano tubes, in: J. Kruis, Y. Tsompanakis, B.H.V. Topping (Eds.), Proc. of the 15th Int. Conf. on Civil, Structural and Environmental Engineering Computing, volume 108, Civil-Comp Press, Stirlingshire, UK, 2015.
[45] S. Gabriele, N.L. Rizzi, V. Varano, A one-dimensional nonlinear thin walled beam model derived from Koiter shell theory, in: B.H.V. Topping, P. Iványi (Eds.), Proc. of the 12th Int. Conf. on Computational Structures Technology, Civil-Comp Press, Stirlingshire, UK, 2014.
[46] N.L. Rizzi, V. Varano, On the postbuckling analysis of thin-walled frames, in: B.H.V. Topping, Y. Tsompanakis (Eds.), Proc. of the 13th Int. Conf. on Civil, Structural and Environmental Engineering Computing, Civil-Comp Press, Stirlingshire, UK, 2011.

Please cite this article in press as: E. Turco, N.L. Rizzi, Pantographic structures presenting statistically distributed defects: Numerical investigations of the effects on deformation fields, Mech. Re. Commun. (2016), http://dx.doi.org/10.1016/j.mechrescom.2016.09.006